Supporting Information

Mechanistic Elucidation of Irreversible Chemodosimetric Sensing of Hydrazine through Structural, Computational, and Bioimaging Analyses

Priyanka Avala[a,b], Malavika S Kumar[a,b], Avijit Kumar Das[a,b*], Ankan Sardar[c], Tilak Raj Maity[d], Aveek Samanta[e], Malay Dolai[f*]

[a] *Department of Chemistry, Christ University, Hosur Road, Bangalore, Karnataka 560029, India, Email: avijitkumar.das@christuniversity.in; sanjuavi.das@gmail.com*
[b] *Centre for Renewable Energy and Environmental Sustainability, Christ University, Karnataka, 560029, India*

[c] *Department of Chemical Sciences, Indian Institute of Science Education and Research (IISER) Kolkata, Mohanpur 741246, India.*
[d] *Department of Biotechnology, Haldia Institute of Technology, Haldia, Purba Medinipur– 721657, West Bengal, India*
[e] *Department of Botany, Prabhat Kumar College, Contai, Purba Medinipur 721404, W.B., India.*
[f] *Department of Chemistry, Prabhat Kumar College, Purba Medinipur 721404, West Bengal, India; E-mail-dolaimalay@yahoo.in*

1 Materials and Instrumentation

General:

Chemicals, solvents including buffer solutions were procured from Sigma Aldrich. Melting points were measured using a hot-plate apparatus with open-ended capillary tubes. 1H NMR and ^13C NMR spectra were recorded on a Bruker Avance 400 MHz spectrometer using DMSO-d6 as the solvent. Chemical shifts and ^1H-^1H coupling constants are reported in δ units and Hertz (Hz), respectively. UV-visible absorption and fluorescence titration experiments were conducted using a PerkinElmer Lambda 30 UV-vis spectrophotometer and a Shimadzu RF-6000 spectrofluorophotometer, respectively, with a 10 mm path length fluorescence cuvette.

2. General method of UV-vis and fluorescence titration:

By UV-vis method:

For UV-vis titrations, stock solution of the sensor was prepared (c = 5.0 x 10^{-5} M) in CH_3CN. Triphosgene solution of concentration c =1 x 10^{-5} M was prepared in CH_3CN and HEPES was added to the solution (9:1 molar ratio). The solution of the guest interfering analytes like Cl^-, Br^-, I^-, F, NO_2^-, AsO_2^{3-}, HSO_4^{2-}, C_2O_4, H_2O_2, NO_3, H_2S, Triethylamine (TEA), NH_3, Ethylenediamine (EDA), Piperidine (Bpy), Hypochlorous acid (HClO), OH^- were also prepared in the order of c =1 x 10^{-5} M. Initially sensor **DBA** solution was prepared by dissolving the sensor in 2 ml acetonitrile followed by the gradual addition of corresponding guest analytes with the particular concentration. Solutions of various concentrations containing sensor and increasing concentrations of analytes were prepared separately. The spectra of these solutions were recorded by means of UV-vis methods.

By fluorescence method:

For fluorescence titrations, stock solution of the sensor (c = 5.0 x 10^{-5} M) was prepared for the titration of analytes in CH_3CN. Initially sensor **DBA** solution was prepared by dissolving the sensor in 2 ml acetonitrile followed by the gradual addition of corresponding guest analytes with the particular concentration. The solution of the guest analytes in the order of 1×10^{-5} M were also prepared. Solutions of various concentrations containing sensor and increasing concentrations of analytes were prepared separately. The spectra of these solutions were recorded by means of fluorescence methods.

Determination of fluorescence quantum yield:

Here, the quantum yield φ was measured by using the following equation,

$$\varphi_x = \varphi_s (F_x / F_s)(A_s / A_x)(n_x^2/ n_s^2)$$

Where,

X & S indicate the unknown and standard solution respectively, φ = quantum yield,

F = area under the emission curve, A = absorbance at the excitation wave length,

n = index of refraction of the solvent. Here φ measurements were performed using anthracene

in ethanol as standard [φ = 0.27] (error ~ 10%).

3. Calculation of the detection limit:

The detection limit (DL) of **DBA** for Hydrazine was determined from the following equation:

DL = K* Sb_1/S

Where K = 2 or 3 (we take 3 in this case); Sb_1 is the standard deviation of the blank solution;

S is the slope of the calibration curve.

From the graph Fig.S1, we get slope = 1668.7, and Sb_1 value is 205.73

Thus, using the formula, we get the Detection Limit for Hydrazine = 0.37 μM.

$$y = 1668.7x + 7881.8$$
$$R^2 = 0.988$$
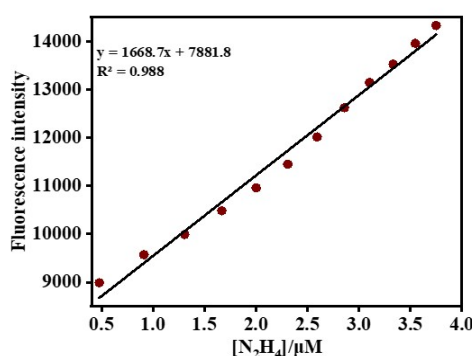
Figure S1. Changes of fluorescence intensity of **DBA** as a function of [N_2H_4]

4. The changes of emission curve of DBA (c = 5.0 × 10^{-5} M) at different time interval by addition of hydrazine (c =1× 10^{-5}) and calculation of first order rate constant:

From the time vs. fluorescent intensity plot at fixed wavelength at 418 nm by using first order rate equation we get the rate constant K = slope × 2.303 = 1.1749× 2.303 = 2.705 Sec^{-1}.

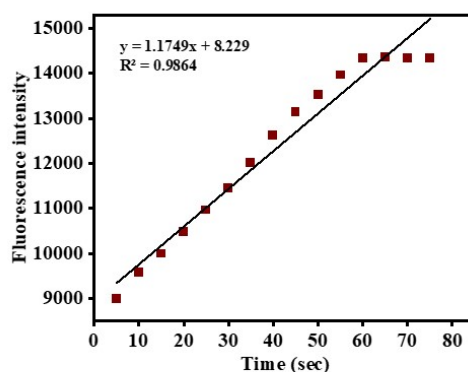$$y = 1.1749x + 8.229$$
$$R^2 = 0.9864$$

Figure S2. The first order rate equation by using Time vs. fluorescent intensity plot at 418 nm.
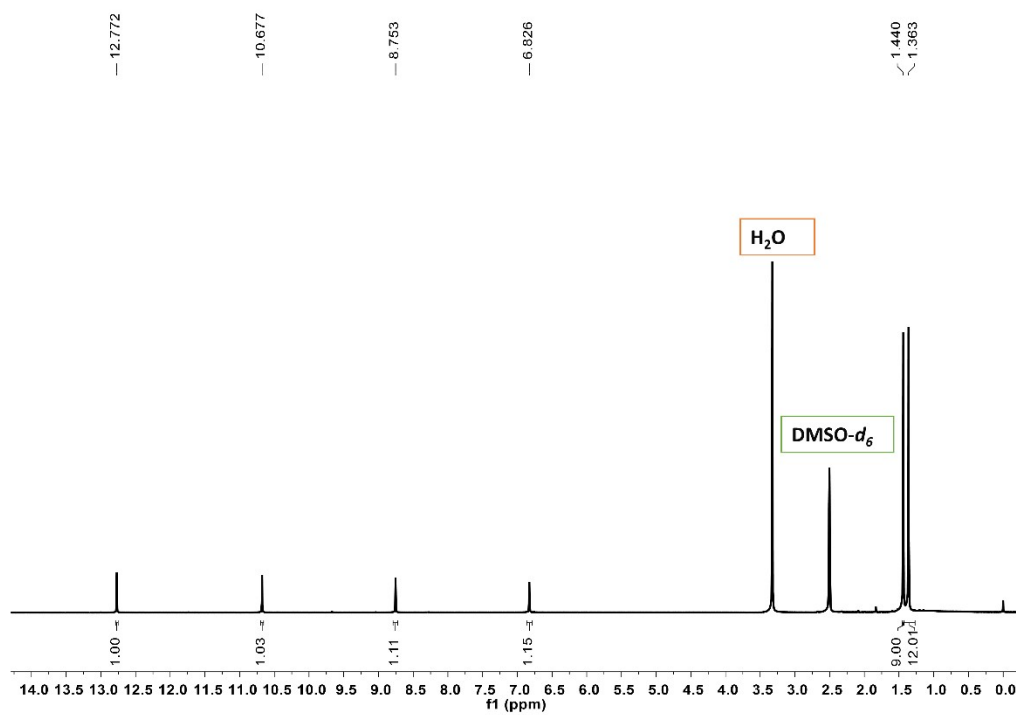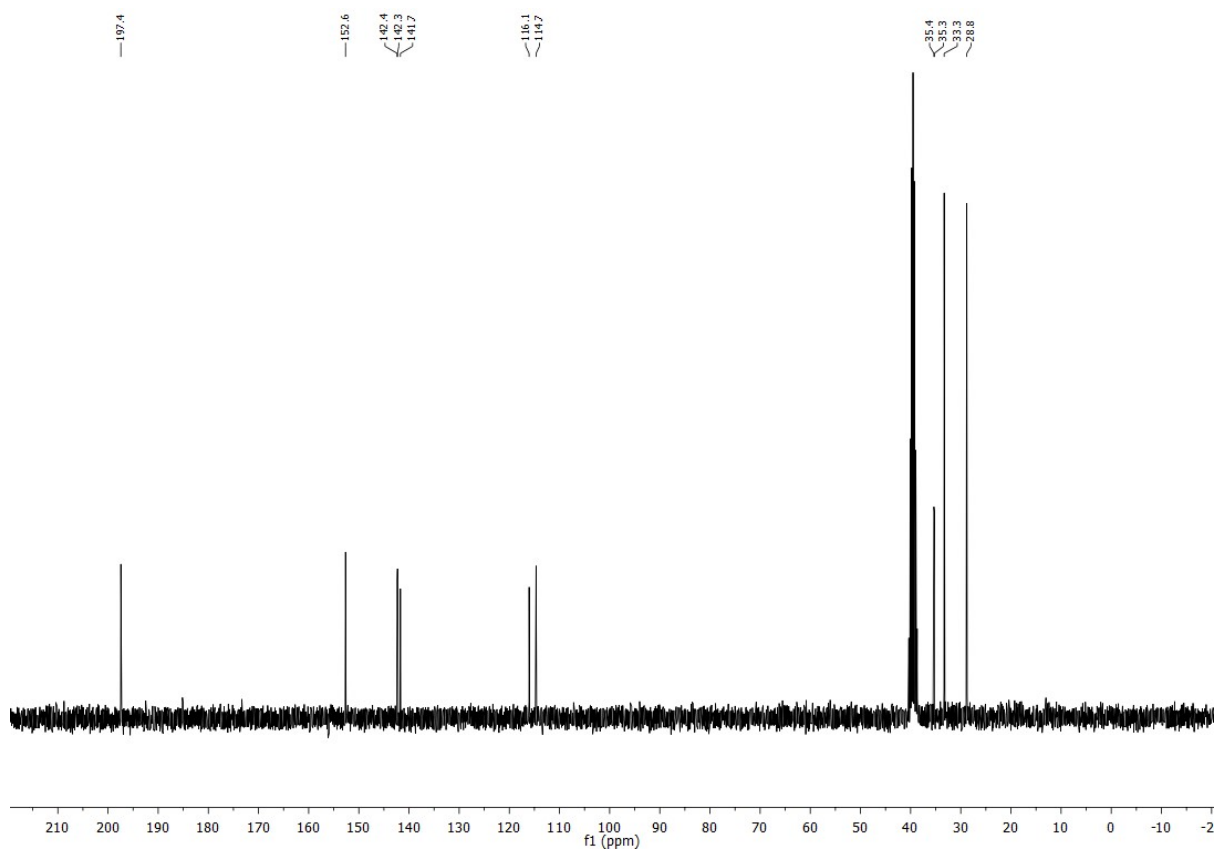
Figure S3. ^{1}H-NMR spectra of **DBA**
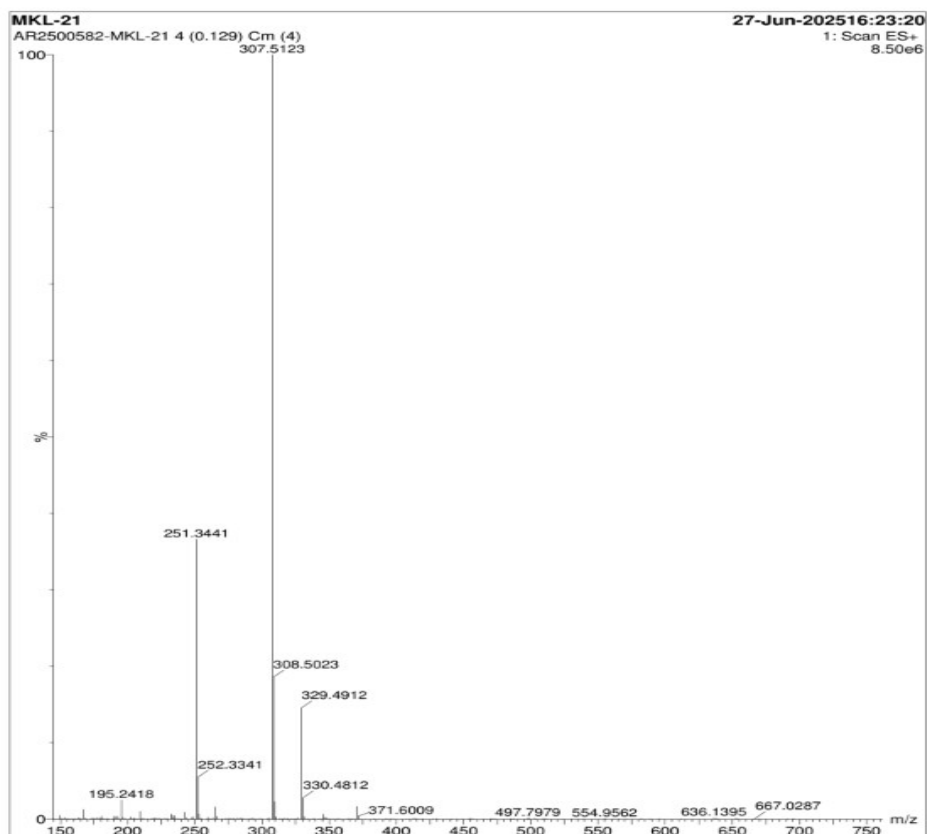

Figure S4. ^{13}C-NMR spectra of **DBA**

Figure S5. Mass spectra of **DBA**
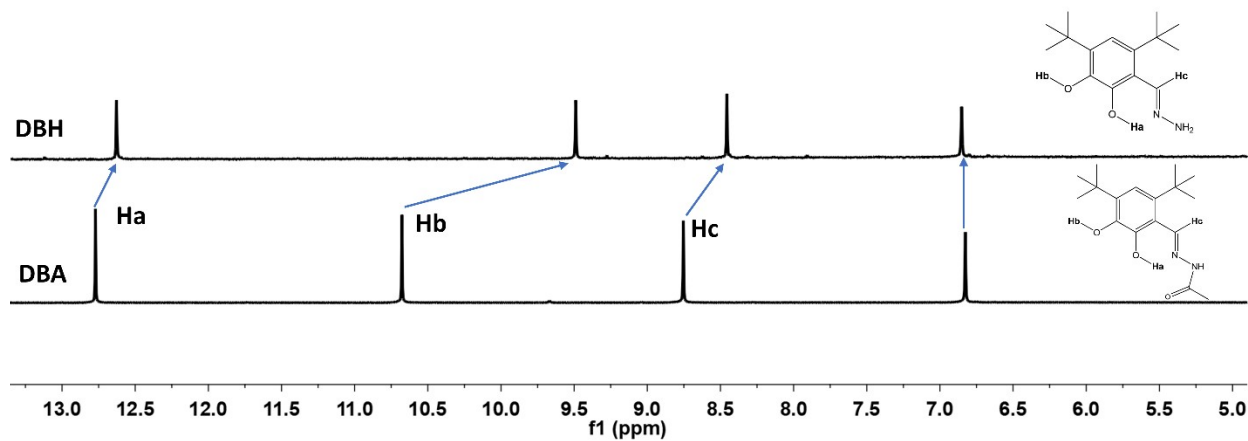
Figure S6. Comparison of ^{1}H-NMR spectra of **DBA** and **DBH** (DBA+N$_2$H$_4$) in DMSO-d^6.
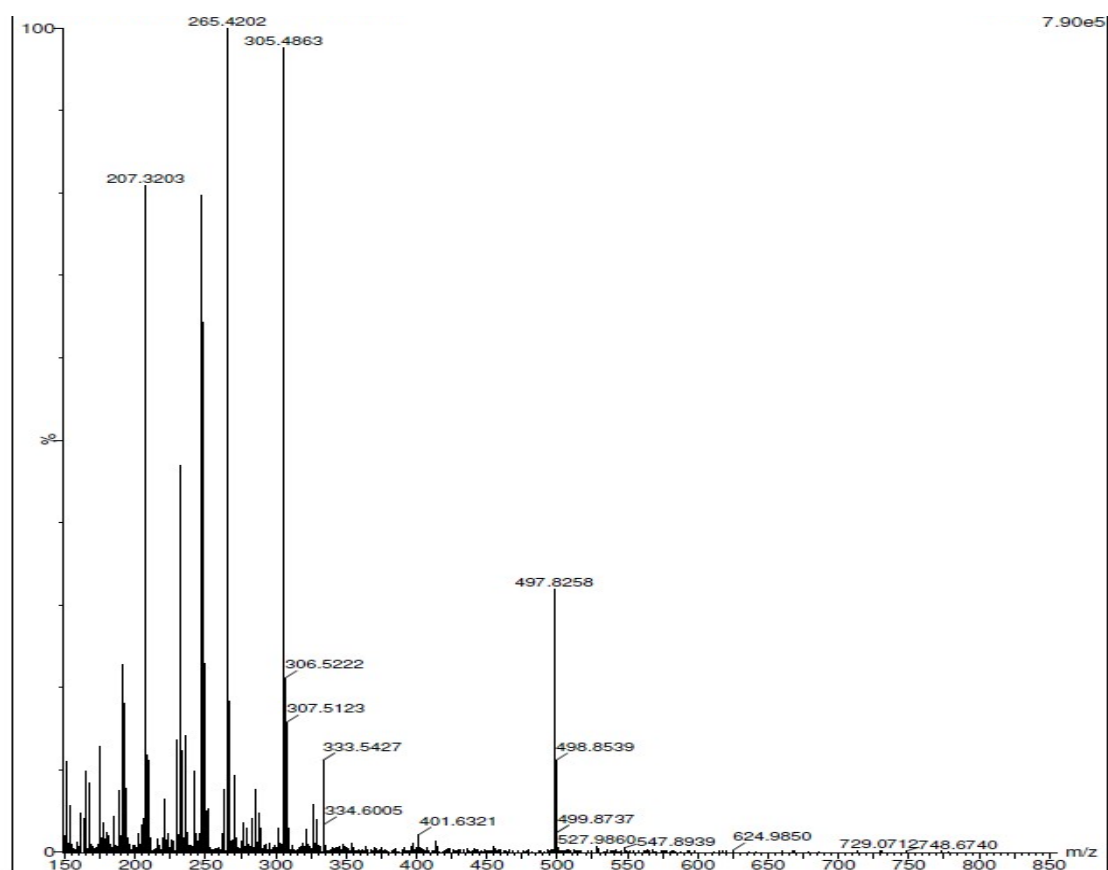
Figure S7. Mass spectra of **DBH** (DBA+N$_2$H$_4$)
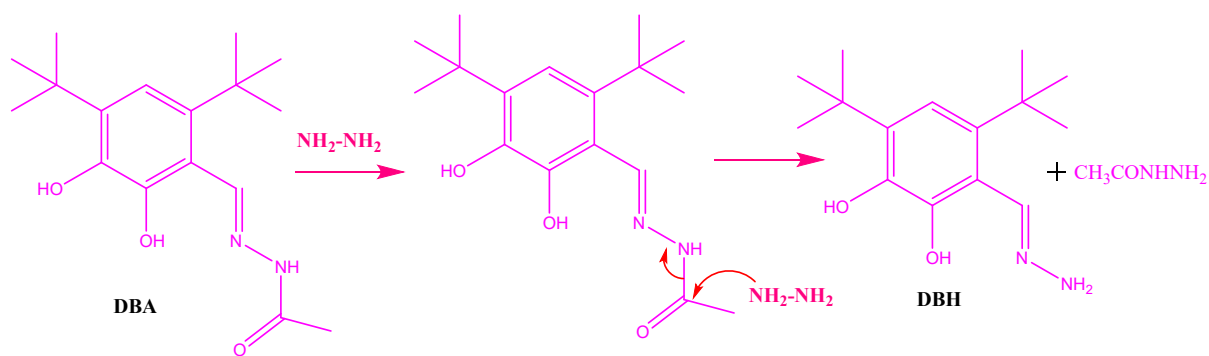
Scheme S1: Probable conversion mechanism of **DBA** to **DBH** (DBA+N$_2$H$_4$)

5. Field soil analysis:

The detection limit DL of **DBA** for Hydrazine in field soil samples was determined to be 0.029 μM.
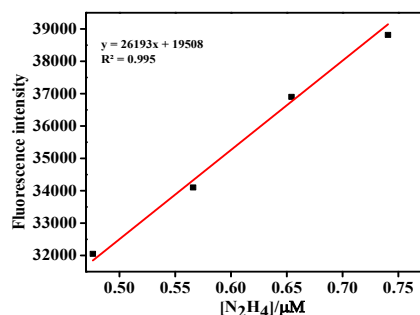

Figure S8. Changes of fluorescence intensity of **DBA** as a function of hydrazine in the field soil sample with error bars ranging 2% (Y error bar for both [±] deviation).
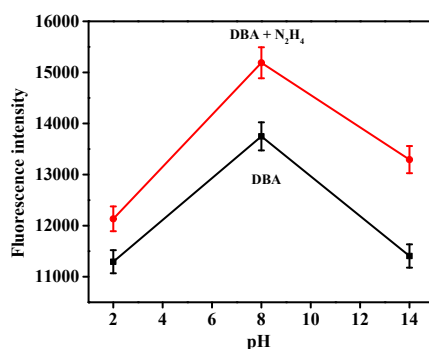
6. pH Effect:

Figure S9. Fluorescence intensity of **DBA** ($c = 5.0 \times 10^{-5}$ M) at various pH values in H_2O, medium in the absence and presence of N_2H_4 with error bars ranging 2% (Y error bar for both [±] deviation).

7. Computational details

Density Functional Theory (DFT)[1] calculations were conducted using the Gaussian 09 (Revision A.02) package, with "Gauss View" utilized for visualizing molecular orbitals. Becke's three-parameter hybrid-exchange functional, the Lee-Yang-Parr expression for nonlocal correlation, and the Vosko-Wilk-Nuair 1980 local correlation functional (B3LYP) were employed in the calculation.[2,3] Optimization of **DBA**
 and **DBH** in the gas phase were performed using the 6-31+(g) basis set. The absorbance spectral properties of **DBA** and **DBH** were calculated by time-dependent density functional

theory (TDDFT)[4-6] associated with the conductor-like polarizable continuum model and we computed the lowest 40 singlet – singlet transition. For H, C, N, O, atoms we used 6-31+(g) basis set for all the calculations. The calculated electron-density plots for frontier molecular orbitals were prepared by using Gauss View 5.1 software. All the calculations were performed with the Gaussian 09W software package.[7]

8. Materials and methods for Root imaging study

Grass pea (*Lathyrus sativus* L.) seeds were surface sterilized with 1% bavistin followed by 0.1% $HgCl_2$ for 5 min and washed in distilled water (3 times, 10 min each). Washed seeds were soaked in distilled water and allowed to germinate in cotton bed for 2 days. The germinated seedlings were then treated with aqueous solutions of 1 mM Hydrazine (N_2H_4) for 2 days and followed 10 µM of **DBA** for 2 days. Sterilized seeds treated with distilled water were marked as control. On 6th day roots from different treatments were washed with distilled water and crushed with 0.1 M potassium phosphate buffer of pH 7 using mortar and pestle. The homogenate was centrifuged (Remi C-24 plus) at room temperature for 10 min at 7,000 rpm and the supernatant was observed the fluorescence under UV light. Transverse section of roots observed under UV light using Zeiss fluorescent microscope.[8,9]
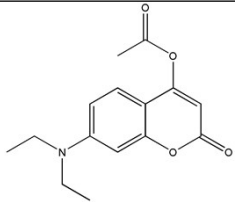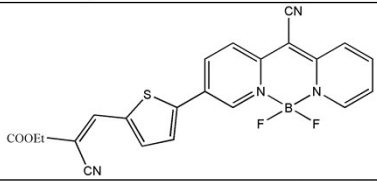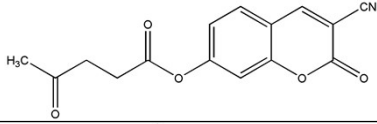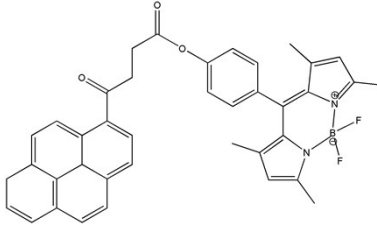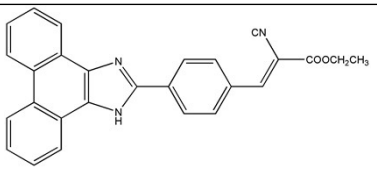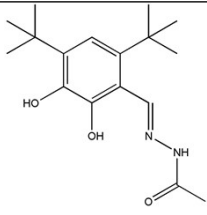
Antioxidant Assay

The radical scavenging activity of **DBA** was determined by using DPPH (2,2-diphenyl-1-picrylhydrazyl) assay according to Baliyan et al. (2022). The decrease in the absorption of the DPPH solution after the addition of an antioxidant was measured at 517 nm. 0.1 mM DPPH solution was prepared by dissolving 2 mg DPPH in 50 ml of ethanol. Different concentrations of **DBA** (10 µM, 20 µM, 30 µM, 40 µM and 50 µM) were added with 0.1 mM DPPH. The reaction mixture was incubated in dark at room temperature for 30 min. After 30 min, the absorbance of the mixture was read at 517 nm. 3 ml of DPPH was taken as control, where ethanol treated as blank. The % radical scavenging activity of **DBA** was calculated using the following formula,

% RSA = [(Abs control - Abs sample) / Abs control] * 100

[Where, RSA is the Radical Scavenging Activity; Abs control is the absorbance of DPPH + ethanol; Abs sample is the absorbance of DPPH + DBA].

9. Table S1: Comparison table of **DBA** with the reported similar type of chemosensors for N$_2$H$_4$ detection

| Ligand	Analyte	Fluorescence response	LOD(μM)	Comparison statements	Ref.
	N$_2$H$_4$	Turn-off	31 μM	(a) Biological application (b) No DFT	[10]
	N$_2$H$_4$	Ratiometric	12 μM	(1) DFT (2) No Biological application	[11]
	N$_2$H$_4$	Turn-on	2.46 μM	(1) No DFT (2) No Biological application	[12]
	N$_2$H$_4$	ON-OFF	1.87 μM	(1) DFT (2) Biological application	[13]
	N$_2$H$_4$	Ratiometric	1.6 μM	(1) Biological application (2) No DFT	[14]
	N$_2$H$_4$	Turn -on	0.37 μM	(1) Ligand crystal structure (2) DFT (3) Biological application (4) Field soil Analysis (5) pH effect	**This work**
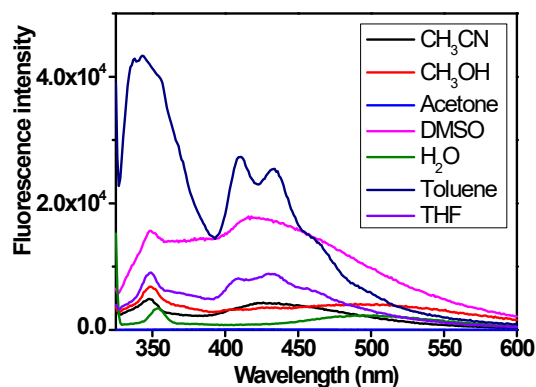
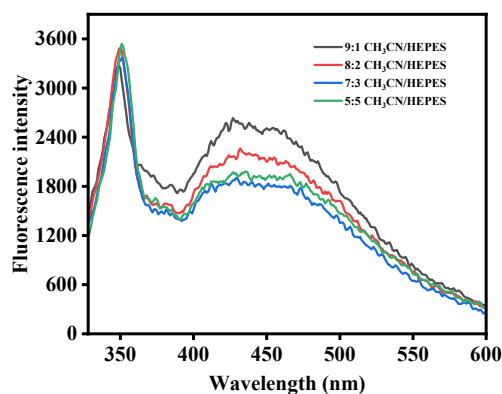**Figure S10.** Changes of emission intensity of **DBA** ($c = 5.0 \times 10^{-5}$ M) in different solvents.

Figure S11. Changes of emission intensity of **DBA** ($c = 5.0 \times 10^{-5}$ M) in presence of different ratios of CH$_3$CN/HEPES buffer.
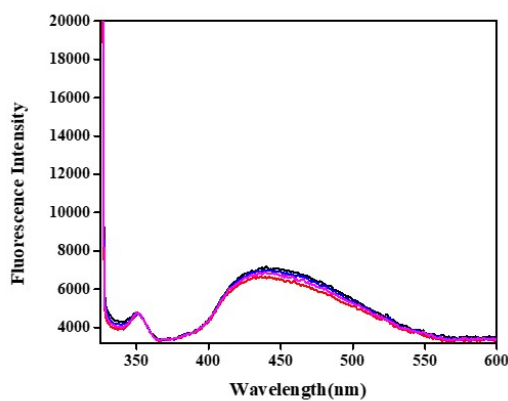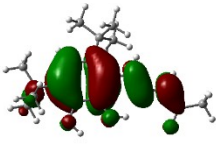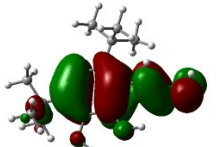

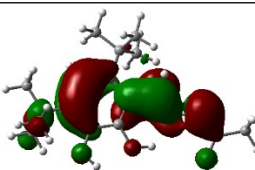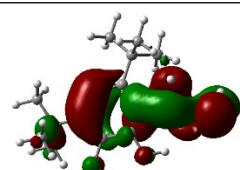**Figure S12.** Changes of emission intensity of **DBA** ($c = 5.0 \times 10^{-5}$ M) in CH$_3$CN/HEPES buffer (5:5, v/v, pH 7.4) solution with 10 equiv. of N$_2$H$_4$ ($c = 1.0 \times 10^{-5}$ M) upon excitation wavelength at 315 nm.
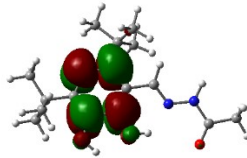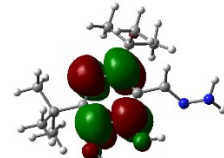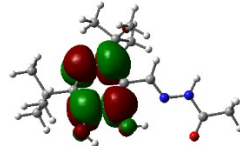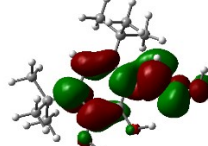
10. Table S2: Main calculated optical transition for **DBA** and **DBH** with composition in terms of molecular orbital contribution of the transition, vertical excitation energies (E).

	DBA	**DBH** (DBA+N$_2$H$_4$)
HOMO-1	E= -8.76 eV	E= -8.78 eV
HOMO-2	E= -10.16 eV	E= - 9.87
LUMO+1	E = 0.48 eV	E = 0.44 eV
LUMO+2	E = 0.58 eV	E = 0.92 eV

11. References:

[1] R. G. Parr and W. Yang, *Density Functional Theory of Atoms and Molecules*, Oxford University Press, Oxford, 1989.

[2] A. D. Becke, *J. Chem. Phys.,* 1993, **98**, 5648.

[3] C. Lee, W. Yang and R. G. Parr, *Phys. Rev. B*, 1998, **37**, 785.

[4] M. E. Casida, C. Jamoroski , K. C. Casida and D. R. Salahub,*J. Chem. Phys.,* 1998, **108**, 4439;

[5] R. E. Stratmann, G. E. Scuseria, M. J. Frisch, *J. Chem. Phys.,* 1998, **109**, 8218;

[6] R. Bauernschmitt and R. Ahlrichs, *Chem. Phys. Lett.,* 1996, **256**, 454.

[7] M. J. Frisch, G. W. Trucks, H. B. Schlegel, G. E. Scuseria, M. A. Robb, J. R. Cheeseman, G. Scalmani, V. Barone, B. Mennucci, G. A. Petersson, H. Nakatsuji, M. Caricato, X. Li, H. P. Hratchian, A. F. Izmaylov, J. Bloino, G. Zheng, J. L. Sonnenberg, M. Hada, M. Ehara, K. Toyota, R. Fukuda, J. Hasegawa, M. Ishida, T. Nakajima, Y. Honda, O. Kitao, H. Nakai, T. Vreven, J. A. Montgomery Jr., J. E. Peralta, F. Ogliaro, M. Bearpark, J. J. Heyd, E. Brothers, K. N. Kudin, V. N. Staroverov, R. Kobayashi, J. Normand, K. Raghavachari, A. Rendell, J. C.

Burant, S. S. Iyengar, J. Tomasi, M. Cossi, N. Rega, J. M. Millam, M. Klene, J. E. Knox, J. B. Cross, V. Bakken, C. Adamo, J. Jaramillo, R. Gomperts, R. E. Stratmann, O. Yazyev, A. J. Austin, R. Cammi, C. Pomelli, J. W. Ochterski, R. L. Martin, K. Morokuma, V. G. Zakrzewski, G. A. Voth, P. Salvador, J. J. Dannenberg, S. Dapprich, A. D. Daniels, Ö. Farkas, J. B. Foresman, J. V Ortiz, J. Cioslowski and D. J. Fox, Gaussian Inc., 2009, Wallingford CT.

[8] Saha S, Das S, Sahoo P (2019) Highly Selective Optical and Fluorescence "Turn On" Signaling of Al^{3+}: Cell Imaging and Estimation in Rice Plant. Chemistry Select, 4(47):13968-73.

[9] Samanta A, Banerjee S, Maity TR, Jahnavi J, Datta S (2022) Towards establishment of a plant-based model to assess the novel anti-cancerous lead molecule (s): An in silico, in vivo and in vitro assessment of some potential anti-cancerous drugs on Lathyrus sativus L. Protoplasma, 259(6):1455-66.

[10] X. Shi, F. Huo, J. Chao and C. Yin, *Sens. Actuators B Chem.*, 2018, **260**, 609–616

[11] Y.-D. Lin and T. J. Chow, *RSC Adv.*, 2013, **3**, 17924.

[12] M. G. Choi, J. Hwang, J. O. Moon, J. Sung and S.-K. Chang, *Org. Lett.*, 2011, **13**, 5260–5263.

[13] A. K. Mahapatra, R. Maji, K. Maiti, S. K. Manna, S. Mondal, S. S. Ali, S. Manna, P. Sahoo, S. Mandal, M. R. Uddin and D. Mandal, *RSC Adv.*, 2015, **5**, 58228–58236.

[14] Z. Li, W. Zhang, C. Liu, M. Yu, H. Zhang, L. Guo and L. Wei, *Sens. Actuators B Chem.*, 2017, **241**, 665–671.